

Single-Event Effects Test Report of the TPS7H4010-SEP Synchronous Step-Down Converter



1 Abstract

The purpose of this study is to characterize the single-event-effects (SEE) performance due to heavy-ion irradiation of the TPS7H4010-SEP. SEE performance was verified at two common output voltage rails of 1.8V and 3.3V. Heavy-ions ranging from an LET_{EFF} of 1.33 to 43 MeV·cm²/mg were used to irradiate 10 production devices. Flux of $\approx 10^4$ and 10^5 ions/cm²·s and fluences of $\approx 10^6$ and 10^7 ions/cm² per run were used for the characterization. The results demonstrated that the TPS7H4010-SEP is SEL and SEB/SEGR-free up to 43 MeV·cm²/mg, at T = 125°C and T = 10°C, respectively, and across the full electrical specifications. SET and SEFI performance for output voltage excursions $\geq |3\%|$ from the nominal voltage and PGOOD $\leq V_{OUT}/2$ are presented and discussed.

Table of Contents

1 Abstract	1
2 Introduction	3
3 Single-Event Effects (SEE)	4
4 Device and Test Board Information	5
5 Irradiation Facility and Setup	8
6 Depth, Range, and LET_{EFF} Calculation	10
7 Test Setup and Procedures	12
8 Destructive Single-Event Effects (DSEE)	14
8.1 Single-Event Latch-up (SEL) Results.....	14
8.2 Single-Event Burnout (SEB) and Single-Event Gate Rupture (SEGR) Results.....	14
9 Single-Event Transients (SET)	16
10 Event Rate Calculations	21
11 Summary	23
12 Revision History	23
A Total Ionizing Dose from SEE Experiments	23
B References	23

List of Figures

Figure 4-1. Photograph of Delidded TPS7H4010-SEP [Left] and Pinout Diagram [Right].....	5
Figure 4-2. TPS7H4010-SEP Board Top View.....	6
Figure 4-3. TPS7H4010EVM Schematic for $V_{OUT} = 3.3\text{ V}$	7
Figure 4-4. TPS7H4010EVM Schematic for $V_{OUT} = 1.8\text{ V}$	7
Figure 5-1. Photograph of the TPS7H4010-SEP Evaluation Board Mounted in Front of the Heavy-Ion Beam Exit Port at the Texas A&M Cyclotron.....	9
Figure 6-1. Generalized Cross-Section of the LBC8 Technology BEOL Stack on the TPS7H4010-SEP [Left] and SEUSS 2020 Application Used to Determine Key Ion Parameters [Right].....	10
Figure 6-2. LET_{EFF} vs Range for ^{84}Kr at the Conditions Used for the SEE Test Campaign.....	11
Figure 7-1. Block Diagram of SEE Test Setup With the TPS7H4010-SEP.....	13
Figure 8-1. Current vs Time for Run # 1 of the TPS7H4010-SEP at $T = 125^{\circ}\text{C}$	14
Figure 8-2. Current vs Time for Run # 5 (Enabled) for the TPS7H4010-SEP at $T = 10^{\circ}\text{C}$	15
Figure 8-3. Current vs Time for Run # 6 (Disabled) for the TPS7H4010-SEP at $T = 10^{\circ}\text{C}$	15
Figure 9-1. Weibull FITs for each V_{OUT} case.....	19
Figure 9-2. Histogram of the Normalized Amplitude for the Positive and Negative V_{OUT} SETs on Run # 9.....	19
Figure 9-3. Histogram of the Normalized Amplitude for the Positive and Negative V_{OUT} SETs on Run # 10.....	19
Figure 9-4. Histogram of the Transient Time for V_{OUT} SETs on Run # 9.....	20
Figure 9-5. Histogram of the Transient Time for V_{OUT} SETs on Run # 10.....	20
Figure 9-6. Histogram of the Transient Time for SS SETs on Run # 9.....	20
Figure 9-7. Histogram of the Transient Time for SS SETs on Run # 10.....	20
Figure 9-8. Worst Case Positive and Negative Polarity $V_{OUT_{SET}}$ for Run # 9.....	20
Figure 9-9. Typical V_{OUT} During a SS_{SEFI} for Run # 9.....	20
Figure 9-10. Typical $PGOOD_{SET} \leq 0.9\text{ V}$ for Run # 9.....	20
Figure 9-11. Worst Case Positive and Negative Polarity $V_{OUT_{SET}}$ for Run # 10.....	20
Figure 9-12. Typical V_{OUT} During a SS_{SET} for Run # 10.....	21
Figure 9-13. Typical $PGOOD_{SET} \leq 1.6\text{ V}$ for Run # 10.....	21

List of Tables

Table 2-1. Overview Information.....	3
Table 6-1. Krypton Ion LET_{EFF} , Depth, and Range in Silicon.....	10
Table 7-1. Equipment Set and Parameters Used for SEE Testing the TPS7H4010-SEP.....	12
Table 8-1. Summary of TPS7H4010-SEP SEL Test Condition and Results.....	14
Table 8-2. Summary of TPS7H4010-SEP SEB Test Condition and Results.....	15
Table 9-1. Summary of TPS7H4010-SEP SET Test Condition and Results ($V_{IN} = 5\text{ V}$ and $V_{OUT} = 1.8\text{ V}$).....	16
Table 9-2. Summary of TPS7H4010-SEP SET Test Condition and Results ($V_{IN} = 12\text{ V}$ & $V_{OUT} = 3.3\text{ V}$).....	17
Table 9-3. Upper Bound Cross Section for $V_{OUT} = 1.8\text{ V}$ at 95% Confidence Interval and Room Temperature.....	17
Table 9-4. Upper Bound Cross Section for $V_{OUT} = 3.3\text{ V}$ at 95% Confidence Interval and Room Temperature.....	18
Table 9-5. Weibull Parameters for $V_{OUT} = 1.8\text{ V}$ and 3.3 V Cases.....	18
Table 10-1. SEL Event Rate Calculations for Worst-Week LEO and GEO Orbits.....	21
Table 10-2. SEB/SEGR Event Rate Calculations for Worst-Week LEO and GEO Orbits.....	21
Table 10-3. Combined SET (1.8V) Event Rate Calculations for Worst-Week LEO and GEO Orbits.....	21
Table 10-4. V_{OUT} SET (1.8V) Event Rate Calculations for Worst-Week LEO and GEO Orbits.....	21
Table 10-5. SS SEFI (1.8V) Event Rate Calculations for Worst-Week LEO and GEO Orbits.....	21
Table 10-6. Combined SET (3.3V) Event Rate Calculations for Worst-Week LEO and GEO Orbits.....	22
Table 10-7. V_{OUT} SET (3.3V) Event Rate Calculations for Worst-Week LEO and GEO Orbits.....	22
Table 10-8. SS SEFI (3.3V) Event Rate Calculations for Worst-Week LEO and GEO Orbits.....	22

Trademarks

All trademarks are the property of their respective owners.

2 Introduction

The TPS7H4010-SEP is a space-enhanced-plastic, 3.5V to 32V input, 6A, synchronous step-down voltage converter. The device provides exceptional efficiency and output accuracy in a very small solution size. Peak current-mode control is employed. Additional features such as adjustable switching frequency, synchronization to an external clock, FPWM option, power-good flag, precision enable, adjustable soft start, and tracking provide both flexible and easy-to-use solutions for a wide range of applications.

The TPS7H4010-SEP requires few external components and has a pinout designed for simple PCB layout with optimal EMI and thermal performance. Protection features include thermal shutdown, input undervoltage lockout, cycle-by-cycle current limiting, and hiccup short-circuit protection. The device is offered in a 30-pin WQFN plastic package. General device information and test conditions are listed in [Table 2-1](#). For more detailed technical specifications, user-guides, and application notes please go to [TPS7H4010-SEP product page](#).

Table 2-1. Overview Information

DESCRIPTION ⁽¹⁾	DEVICE INFORMATION
TI Part Number	TPS7H4010-SEP
Orderable Number	TPS7H4010MRNPTSEP
Device Function	Point-of-load (POL) Switching Regulator
Technology	Linear BiCMOS 8 (LBC8)
Exposure Facility	Radiation Effects Facility, Cyclotron Institute, Texas A&M University (25 MeV/nucleon)
Heavy Ion Fluence per Run	$5.65 \times 10^5 - 1 \times 10^7$ ions/cm ²
Irradiation Temperature	10°C (for SEB/SEGR testing), 25°C (for SET testing), and 125°C (for SEL testing)

- (1) TI may provide technical, applications or design advice, quality characterization, and reliability data or service, providing these items shall not expand or otherwise affect TI's warranties as set forth in the Texas Instruments Incorporated Standard Terms and Conditions of Sale for Semiconductor Products and no obligation or liability shall arise from Semiconductor Products and no obligation or liability shall arise from TI's provision of such items.

3 Single-Event Effects (SEE)

The primary concern for the TPS7H4010-SEP is the robustness against destructive single-event effects (DSEE): single-event latch-up (SEL), single-event burnout (SEB), and single-event gate rupture (SEGR). In mixed technologies such as the BiCMOS process used on the TPS7H4010-SEP, the CMOS circuitry introduces a potential for SEL susceptibility.

SEL can occur if excess current injection caused by the passage of an energetic ion is high enough to trigger the formation of a parasitic cross-coupled PNP and NPN bipolar structure (formed between the p-sub and n-well and n+ and p+ contacts) [1,2]. The parasitic bipolar structure initiated by a single-event creates a high-conductance path (inducing a steady-state current that is typically orders-of-magnitude higher than the normal operating current) between power and ground that persists (is "latched") until power is removed, the device is reset, or until the device is destroyed by the high-current state. The TPS7H4010-SEP was tested for SEL at the maximum recommended voltage of 32 V, maximum load current of 6 A, and V_{OUT} of 3.3 and 1.8 V. The device exhibited no SEL with heavy-ions with $LET_{EFF} = 43 \text{ MeV}\cdot\text{cm}^2/\text{mg}$ at flux $\approx 10^5 \text{ ions/cm}^2\cdot\text{s}$, fluences of $\approx 10^7 \text{ ions/cm}^2$, and a die temperature of 125°C.

Since this device is designed to conduct large currents (up to 6 A) and withstand up to 32 V during the off-state, the power LDMOS introduces a potential susceptibility for SEB and SEGR [2]. The TPS7H4010-SEP was evaluated for SEB/SEGR at full load conditions of 6 A, and a maximum voltage of 32 V in both the enabled and disabled modes. Because it has been shown that MOSFET susceptibility to burnout decreases with temperature [2], the device was evaluated while operating under sub-ambient temperatures. The devices were cooled-down (or "chilled") by using VORTEC tube (model 611). During the SEB/SEGR testing, not a single current event was observed, demonstrating that the TPS7H4010-SEP is SEB/SEGR-free up to $LET_{EFF} = 43 \text{ MeV}\cdot\text{cm}^2/\text{mg}$ at a flux of $\approx 10^5 \text{ ions/cm}^2\cdot\text{s}$, fluences of $\approx 10^7 \text{ ions/cm}^2$, and a die temperature of $\approx 10^\circ\text{C}$.

The TPS7H4010-SEP was characterized for SET and SEFIs at flux of $\approx 10^4 \text{ ions/cm}^2\cdot\text{s}$, fluences of $3 \times 10^6 \text{ ions/cm}^2$, at room temperature. The device was characterized at $P_{VIN} = 12 \text{ V}$ to $V_{OUT} = 3.3 \text{ V}$ and $P_{VIN} = 5 \text{ V}$ to $V_{OUT} = 1.8 \text{ V}$ at full load of 6-A. Under these conditions the device showed 2 different single-event transients (SET) signatures and 1 single-event functional interrupt (SEFI) under heavy-ion irradiation. All observed types of SETs were self-recoverable without the need of external intervention. The observed transients can be classified as:

1. A brief transient of the output voltage (refer here as V_{OUT_SET}). For the purpose of this report the transients were characterized for deviations $-3\% \leq V_{OUT} \leq 3\%$ from the nominal output voltage of 1.8 V ($\pm 54 \text{ mV}$) and 3.3 V ($\pm 99 \text{ mV}$). The upsets typically have duration of 30 μs and peak normalized deviation of 4.3% from the nominal voltage. For more details please refer to [Section 9](#).
2. A soft-start power re-cycle which results in the V_{OUT} dropping to zero volts and characterized by a long recovery time governed by the soft start (SS) capacitor. This kind of SEFI is referred to here as SS_{SEFI} .
3. A PGOOD upset $\geq 10\%$ from the nominal output voltage.

4 Device and Test Board Information

The TPS7H4010-SEP is packaged in a 30-pin WQFN plastic package as shown in [Figure 4-1](#). The TPS7H4010EVM evaluation board was used to evaluate the performance and characteristics of the TPS7H4010-SEP under heavy-ions. [Figure 4-2](#) shows the top view of the evaluation board used for the radiation testing. [Figure 4-3](#) and [Figure 4-4](#) shows the EVM board schematics for the $V_{OUT} = 3.3\text{ V}$ and $V_{OUT} = 1.8\text{ V}$ used for the heavy-ion testing campaign. See the [TPS7H4010-SP Evaluation Module user's guide](#) for more information about the evaluation board.

The package was delidded to reveal the die face for all heavy-ion testing.

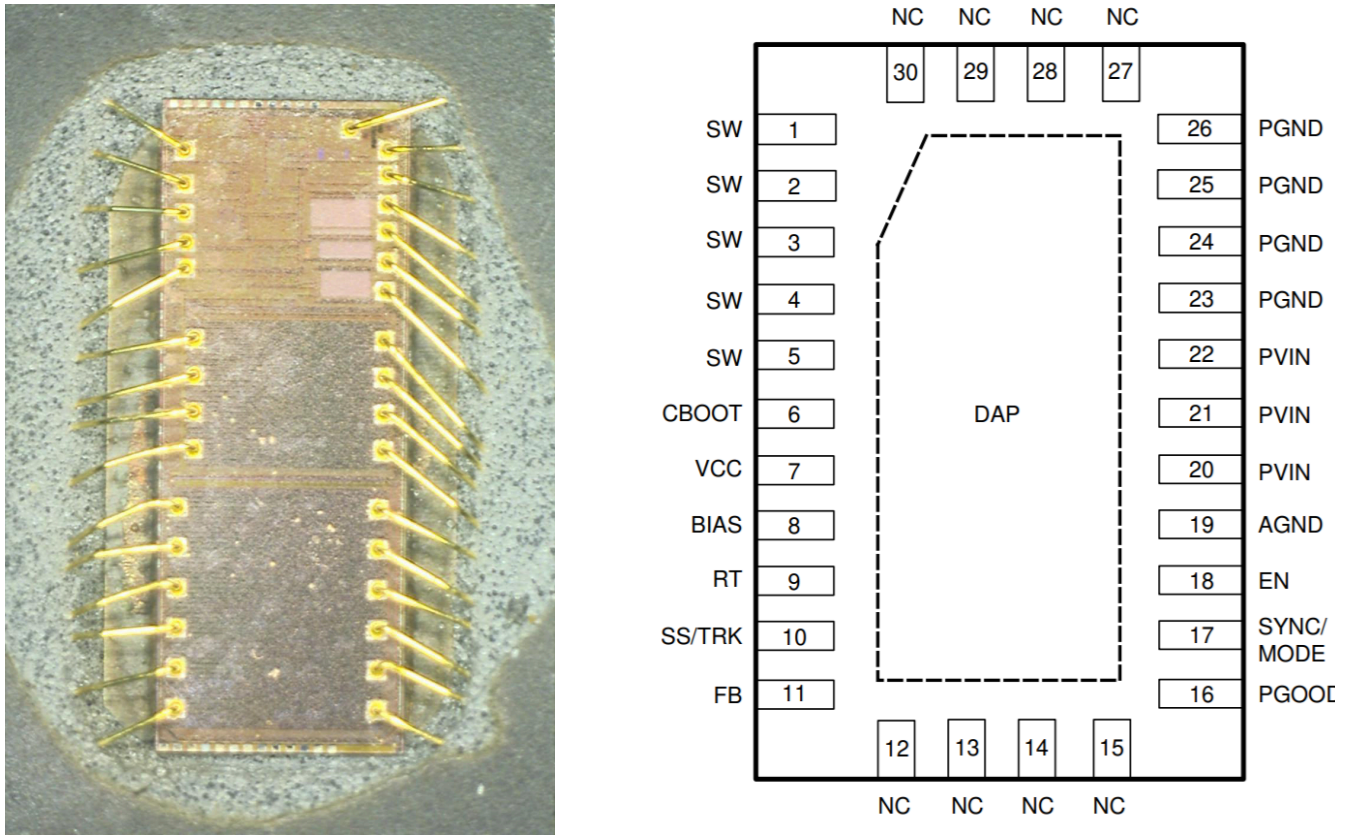


Figure 4-1. Photograph of Delidded TPS7H4010-SEP [Left] and Pinout Diagram [Right]

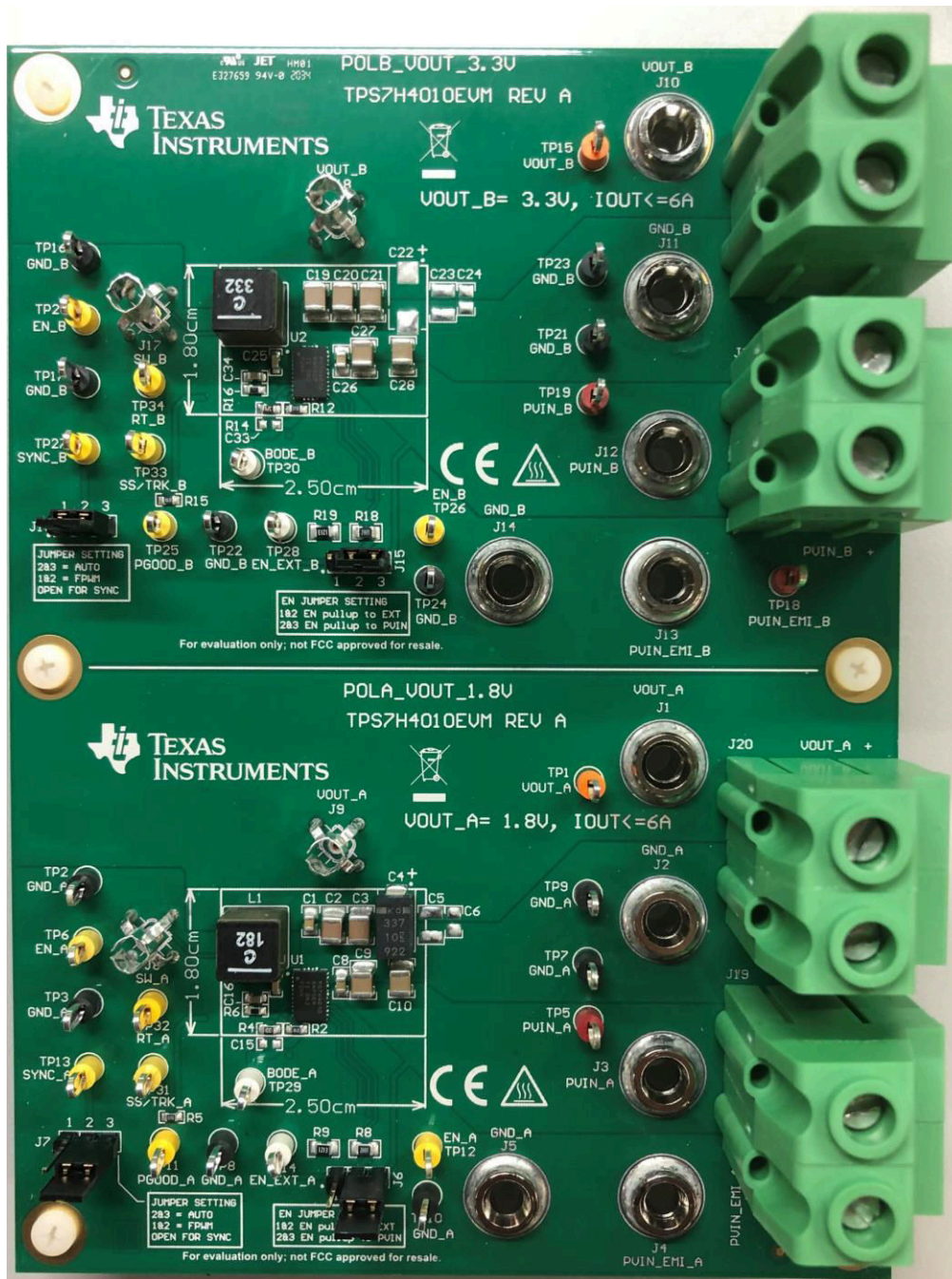


Figure 4-2. TPS7H4010-SEP Board Top View

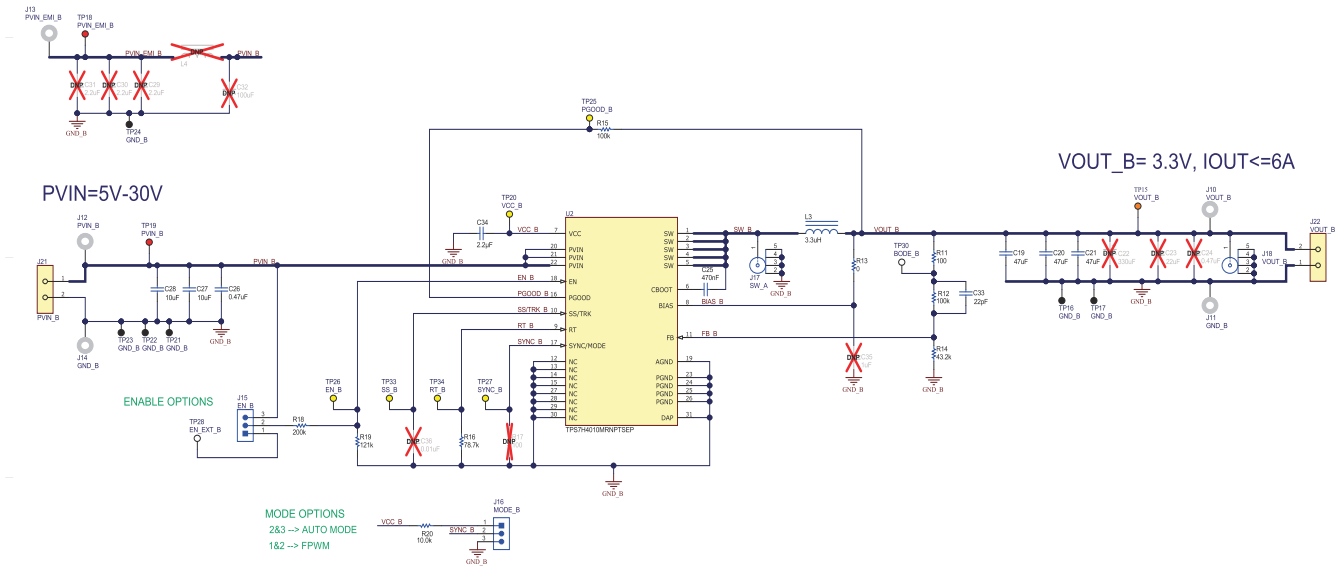


Figure 4-3. TPS7H4010EVM Schematic for $V_{OUT} = 3.3\text{ V}$

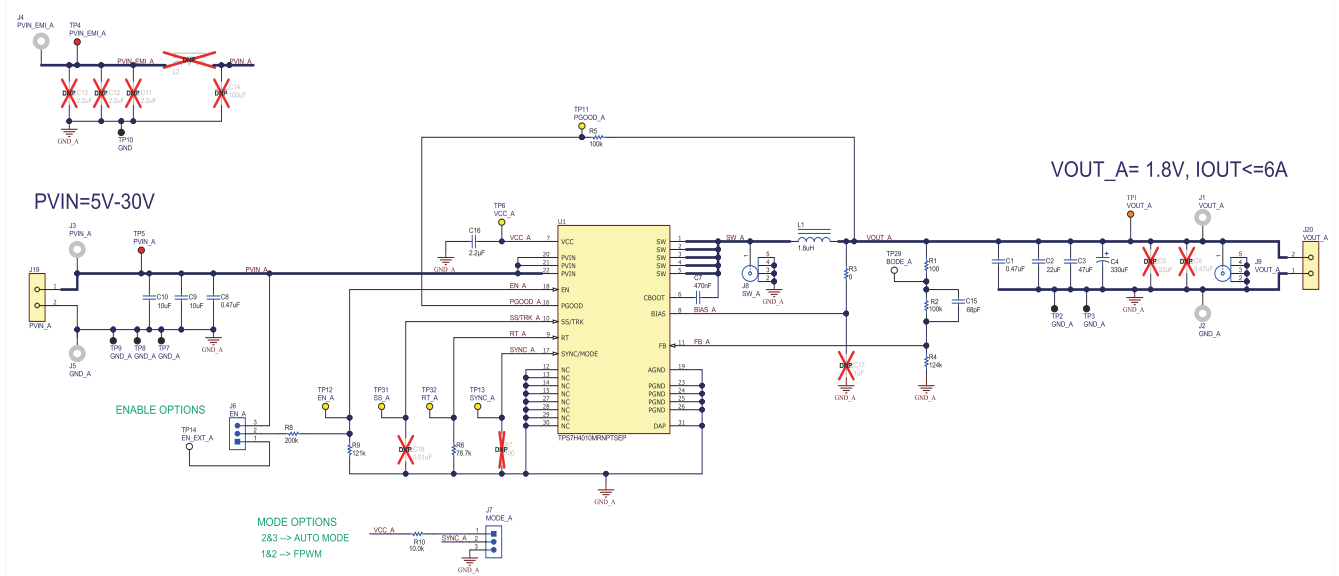


Figure 4-4. TPS7H4010EVM Schematic for $V_{OUT} = 1.8\text{ V}$

5 Irradiation Facility and Setup

The heavy-ion species used for the SEE studies on this product were provided and delivered by the TAMU Cyclotron Radiation Effects Facility using a superconducting cyclotron and an advanced electron cyclotron resonance (ECR) ion source. At the fluxes used, ion beams had good flux stability and high irradiation uniformity over a 1-in diameter circular cross-sectional area for the in-air station. Uniformity is achieved by magnetic defocusing. The flux of the beam is regulated over a broad range spanning several orders of magnitude. For the bulk of these studies, ion flux of 10^4 and 10^5 ions/cm²·s were used to provide heavy-ion fluences of $\approx 3 \times 10^6$ and 10^7 ions/cm².

For the experiments conducted in this report the following ions and corresponding angles were used in order to provide a range of LET_{EFF} of 1.33 to 43 MeV·cm² /mg.

- Krypton (⁸⁴Kr) at 44.3° for an LET_{EFF} = 43 MeV
 - Range_{EFF} = 77.7 μm
 - Total Kinetic Energy = 2.081 GeV (25 MeV/nucleon)
- Krypton (⁸⁴Kr) at 42.7° for an LET_{EFF} = 43.1 MeV
 - Range_{EFF} = 73.6 μm
 - Total Kinetic Energy = 1.259 GeV (15 MeV/nucleon)
- Krypton (⁸⁴Kr) at 0° for an LET_{EFF} = 29.7 MeV
 - Range_{EFF} = 118.2 μm
 - Total Kinetic Energy = 1.259 GeV (15 MeV/nucleon)
- Copper (⁶³Cu) at 41.6° for an LET_{EFF} = 28.1 MeV
 - Range_{EFF} = 80.1 μm
 - Total Kinetic Energy = 0.944 GeV (15 MeV/nucleon)
- Copper (⁶³Cu) at 0° for an LET_{EFF} = 19.7 MeV
 - Range_{EFF} = 124.1 μm
 - Total Kinetic Energy = 0.944 GeV (15 MeV/nucleon)
- Argon (⁴⁰Ar) at 42.3° for an LET_{EFF} = 12 MeV
 - Range_{EFF} = 120.8 μm
 - Total Kinetic Energy = 0.599 GeV (15 MeV/nucleon)
- Argon (⁴⁰Ar) at 0° for an LET_{EFF} = 8.44 MeV
 - Range_{EFF} = 180.9 μm
 - Total Kinetic Energy = 0.599 GeV (15 MeV/nucleon)
- Neon (²⁰Ne) at 43.1° for an LET_{EFF} = 3.89 MeV
 - Range_{EFF} = 177 μm
 - Total Kinetic Energy = 0.300 GeV (15 MeV/nucleon)
- Neon (²⁰Ne) at 0° for an LET_{EFF} = 2.74 MeV
 - Range_{EFF} = 261.3 μm
 - Total Kinetic Energy = 0.300 GeV (15 MeV/nucleon)
- Nitrogen (¹⁴N) at 0° for an LET_{EFF} = 1.33 MeV
 - Range_{EFF} = 371.8 μm
 - Total Kinetic Energy = 0.210 GeV (15 MeV/nucleon)

Ion uniformity for these experiments was between 88 and 98%.

Figure 5-1 shows the TPS7H4010-SEP test board used for the experiments at the TAMU facility. Although not visible in this photo, the beam port has a 1-mil Aramica window to allow in-air testing while maintaining the vacuum within the accelerator with only minor ion energy loss. All through-hole test points were soldered backwards for easy access of the signals while having enough room to change the angle of incidence and maintaining the 40-mm distance to the die. The in-air gap between the device and the ion beam port window was maintained at 40 mm for all runs.

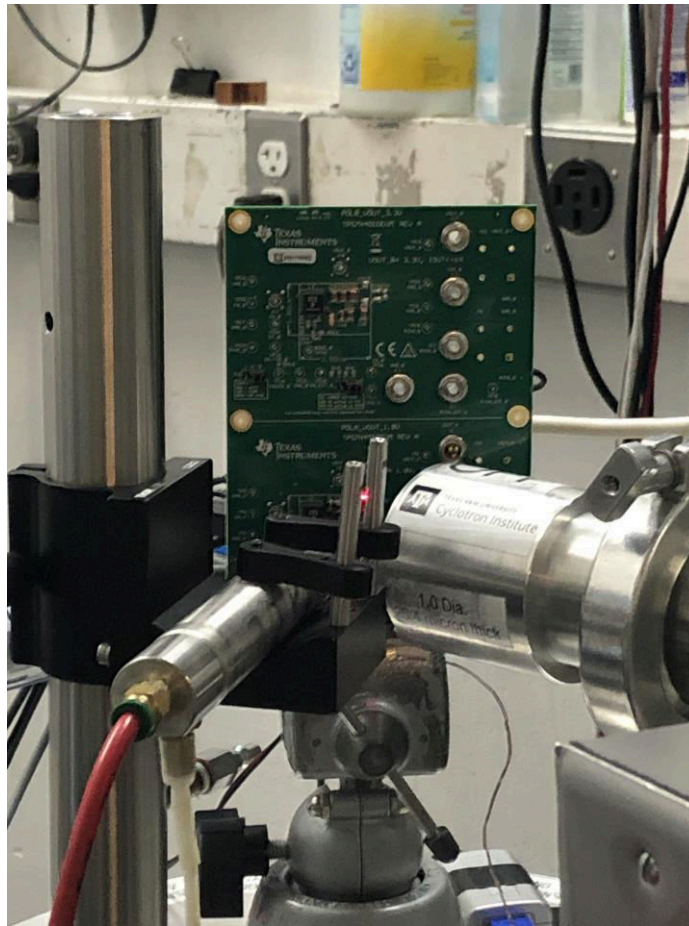


Figure 5-1. Photograph of the TPS7H4010-SEP Evaluation Board Mounted in Front of the Heavy-Ion Beam Exit Port at the Texas A&M Cyclotron

6 Depth, Range, and LET_{EFF} Calculation

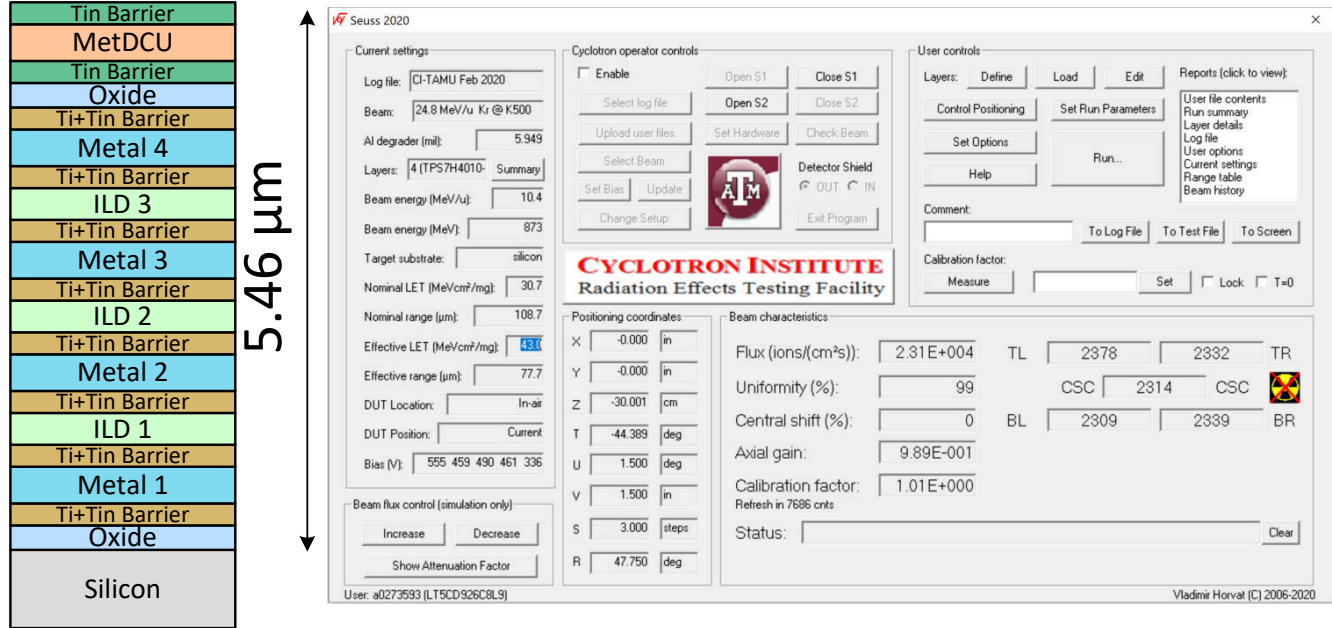


Figure 6-1. Generalized Cross-Section of the LBC8 Technology BEOL Stack on the TPS7H4010-SEP [Left] and SEUSS 2020 Application Used to Determine Key Ion Parameters [Right]

The TPS7H4010-SEP is fabricated in the TI Linear BiCMOS 180-nm process with a back-end-of-line (BEOL) stack consisting of 4 levels of standard thickness aluminum metal on a 0.6-μm pitch. The total stack height from the surface of the passivation to the silicon surface is 5.46 μm based on nominal layer thickness as shown in Figure 6-1. Accounting for energy loss through the 1-mil thick Aramica beam port window, the 40-mm air gap, and the BEOL stack over the TPS7H4010-SEP, the effective LET (LET_{EFF}) at the surface of the silicon substrate, the depth, and the ion range was determined with the SEUSS 2020 Software (provided by the Texas A&M Cyclotron Institute and based on the latest SRIM-2013 [7] models). The results are shown in Table 6-1. The LET_{EFF} vs range for the ⁸⁴Kr heavy-ion is shown on Figure 6-2. The stack was modeled as a homogeneous layer of silicon dioxide (valid since SiO₂ and aluminum density are similar).

Table 6-1. Krypton Ion LET_{EFF}, Depth, and Range in Silicon

ION TYPE	ANGLE OF INCIDENCE	DEGRADER STEPS (#)	DEGRADER ANGLE	RANGE IN SILICON (μm)	LET _{EFF} (MeV·cm ² /mg)
⁸⁴ Kr	44.38	3	47.75	77.7	43
⁸⁴ Kr	42.7	0	0	73.6	43.1
⁸⁴ Kr	0	0	0	118.2	29.7
⁶³ Cu	41.6	0	0	80.1	28.1
⁶³ Cu	0	0	0	124.1	19.7
⁴⁰ Ar	42.3	0	0	120.8	12
⁴⁰ Ar	0	0	0	180.9	8.44
²⁰ Ne	43.1	0	0	177	3.89
²⁰ Ne	0	0	0	261.3	2.74
¹⁴ N	0	0	0	371.8	1.33

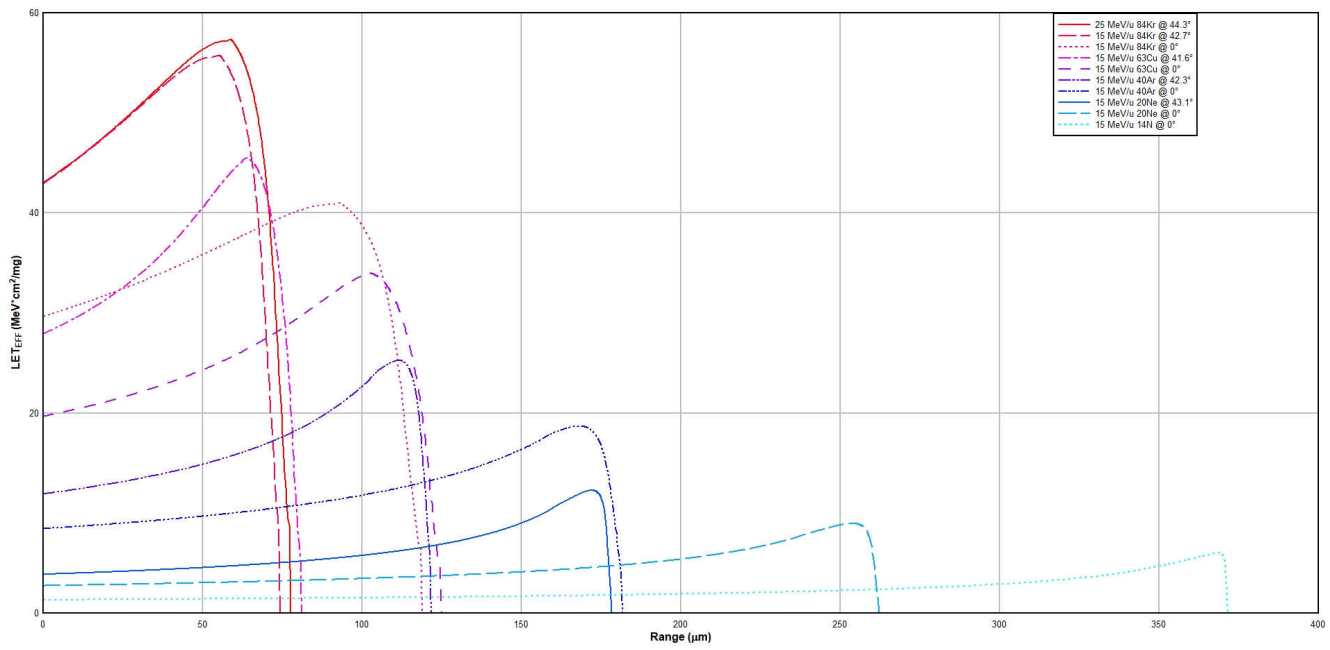


Figure 6-2. LET_{EFF} vs Range for ⁸⁴Kr at the Conditions Used for the SEE Test Campaign

7 Test Setup and Procedures

SEE testing was performed on a TPS7H4010-SEP device mounted on a TPS7H4010EVM. The device power was provided using the J19 (PVIN) and (GND) inputs with the N6766A PS Module mounted on a N6705 precision power supply in a 4-wire configuration. Discrete power resistors of 0.3 Ω ($V_{OUT} = 1.8$ V) and 0.55 Ω ($V_{OUT} = 3.3$ V) were used to load the device to 6 A for the SEE testing campaign. The device was tested under Auto Mode for all runs by tying the SYNC to GND using the J7 jumper.

For SEL, SEB, and SEGR testing, the device was powered up to the maximum recommended operating voltage of 32 V and loaded with the maximum load of 6 A. Two commonly used output voltages, 3.3 and 1.8 V, were used for the SEE testing campaign. For the SEB/SEGR characterization, the device was tested under enabled and disabled modes. The device was disabled by using jumper J6, connecting EN to GND. The discrete load resistor was connected even when the device was disabled to help differentiate if an SET momentarily activated the device under the heavy-ion irradiation. During the SEB/SEGR testing with the device in disabled mode, not a single V_{OUT} transient or input current event was observed.

For the SET characterization, the device was powered up to 12 V for the 3.3-V V_{OUT} case and 5 V for the 1.8-V case. The SET events were monitored using two National Instruments (NI) PXIe-5172 scope cards. One scope was used to monitor and trigger from V_{OUT} , using a window trigger around $\pm 3\%$ from the nominal output voltage. The second scope was used to monitor and trigger from the PGOOD at 1.5 V (for the $V_{OUT} = 1.8$ V) and 3 V (for the $V_{OUT} = 3.3$ V), using a edge/negative trigger. Both scopes were mounted on a NI PXIe-1095 chassis.

All equipment was controlled and monitored using a custom-developed LabVIEW program (PXI-RadTest) running on a HP-Z4 desktop computer. The computer communicates with the PXI chassis via an MXI controller and NI PXIe-8381 remote control module.

Figure 7-1 shows a block diagram of the setup used for SEE testing of the TPS7H4010-SEP. Table 7-1 shows the connections, limits, and compliance values used during the testing. A die temperature of 125°C was used for SEL and was achieved with the use of a convection heat gun aimed at the die. For the SEB/SEGR testing, the device was cooled-down to $\approx 10^\circ\text{C}$ using a VORTEC tube (model: 611), aimed at the die. For SET testing, the device was tested at room temperature (no cooling or heating was applied to the DUT). The die temperature was monitored during all the testing using a T-Type thermocouple attached to the thermal pad vias (on the bottom side of the EVM) with thermal paste. The thermocouple was held in place by using high temperature tape (kapton-tape). Die-to-thermocouple temperature was verified using a IR-camera prior to the SEE test campaign.

Table 7-1. Equipment Set and Parameters Used for SEE Testing the TPS7H4010-SEP

PIN NAME	EQUIPMENT USED	CAPABILITY	COMPLIANCE	RANGE OF VALUES USED
VIN	Agilen N6700 PS (Channel #3)	15 A	10 A	5, 12, and 32 V
Oscilloscope Card on V_{OUT}	NI-PXIe 5172	100 MS/s	—	10 MS/s
Oscilloscope Card on V_{OUT}	NI-PXIe 5172	100 MS/s	—	50 MS/s
Digital I/O	NI-PXIe 6589	—	—	Interrupt Based

All boards used for SEE testing were fully checked for functionality. Dry runs were also performed to ensure that the test system was stable under all bias and load conditions prior to being taken to the TAMU facility. During the heavy-ion testing, the LabVIEW control program powered up the TPS7H4010-SEP device and set the external sourcing and monitoring functions of the external equipment. After functionality and stability was confirmed, the beam shutter was opened to expose the device to the heavy-ion beam. The shutter remained open until the target fluence was achieved (determined by external detectors and counters). During irradiation, the NI scope cards continuously monitored the signals. When the output voltage exceeded the pre-defined 3% window trigger, or when the PG signal changed from High to Low (using a negative edge trigger), a data capture was initiated. In addition to monitoring the voltage levels of the two scopes, VIN current and the +5-V signal from TAMU were

8 Destructive Single-Event Effects (DSEE)

8.1 Single-Event Latch-up (SEL) Results

During SEL characterization, the device was heated using forced hot air, maintaining the DUT temperature at 125°C. The die temperature was monitored during testing using a T-Type thermocouple attached to the thermal pad vias (on the bottom side of the EVM) with thermal paste. The thermocouple was held in-place by using high temperature tape (kapton-tape). Die-to-thermocouple temperature was verified using a IR-camera.

The species used for the SEL testing was a Krypton (^{84}Kr) ion with an angle-of-incidence of 44.38°, degraded by 3-steps of a degrader angle of 47.75° for an $\text{LET}_{\text{EFF}} = 43 \text{ MeV}\cdot\text{cm}^2/\text{mg}$ (for more details refer to [Section 6](#)). The kinetic energy in the vacuum for this ion is 2.081 GeV (25-MeV/amu line). Flux of approximately $10^5 \text{ ions/cm}^2\cdot\text{s}$ and a fluence of approximately 10^7 ions/cm^2 were used for the four runs. Run duration to achieve this fluence was approximately 2 minutes. The two devices were powered up and exposed to the heavy-ions using the maximum recommended voltage of 32 V and maximum load of 6 A. No SEL events were observed during all four runs, indicating that the TPS7H4010-SEP is SEL-free. [Table 8-1](#) shows the SEL test conditions and results. [Figure 8-1](#) shows a plot of the current vs time for run # 1.

Table 8-1. Summary of TPS7H4010-SEP SEL Test Condition and Results

RUN #	UNIT #	ION	LET_{EFF} (MeV·cm ² /mg)	FLUX (ions·cm ² ·s)	FLUENCE (# ions)	V _{OUT} (V)
1	1	^{84}Kr	43	9.79×10^4	9.99×10^6	1.8
2	2	^{84}Kr	43	7.06×10^4	1×10^7	3.3
3	3	^{84}Kr	43	8.56×10^4	9.98×10^6	1.8
4	4	^{84}Kr	43	1.1×10^5	9.97×10^6	3.3

Using the MFTF method described in [Single-Event Effects \(SEE\) Confidence Interval Calculations application report](#) and combining (or summing) the fluences of the four runs @ 125°C (3.99×10^7), the upper-bound cross-section (using a 95% confidence level) is calculated as:

$$\sigma_{\text{SEL}} \leq 9.23 \times 10^{-8} \text{ cm}^2/\text{device for } \text{LET}_{\text{EFF}} = 43 \text{ MeV}\cdot\text{cm}^2/\text{mg and } T = 125^\circ\text{C}.$$

NOTE: The current spikes are due to the output transients on the output voltage.

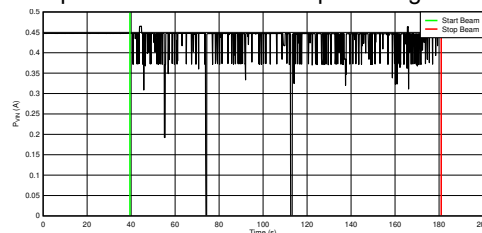


Figure 8-1. Current vs Time for Run # 1 of the TPS7H4010-SEP at T = 125°C

8.2 Single-Event Burnout (SEB) and Single-Event Gate Rupture (SEGR) Results

During the SEB/SEGR characterization, the device was cooled-down using a VORTEC tube (model: 611) to $\approx 10^\circ\text{C}$. The die temperature was monitored during the testing using a T-Type thermocouple attached to the thermal pad vias (on the bottom side of the EVM) with thermal paste. The thermocouple was held in place by using high temperature tape (kapton-tape). Die-to-thermocouple temperature was verified using a IR-camera.

The species used for the SEB/SEGR testing was a Krypton (^{84}Kr) ion with an angle-of-incidence of 44.38°, degraded by 3-steps with a degrader angle of 47.75°, for an $\text{LET}_{\text{EFF}} = 43 \text{ MeV}\cdot\text{cm}^2/\text{mg}$ (for more details refer to [Section 6](#)). The kinetic energy in the vacuum for this ion is 2.081 GeV (25-MeV/amu line). Flux of approximately $10^5 \text{ ions/cm}^2\cdot\text{s}$ and a fluence of approximately 10^7 ions/cm^2 were used for the four runs. Run duration to achieve this fluence was approximately 2 minutes. The two devices were powered up using the recommended maximum voltage of 32 V and the maximum load of 6 A. The TPS7H4010-SEP was tested under enabled and disabled modes, the device was disabled by using jumper J6 connecting EN to GND. The discrete load resistor was connected, even when the device was disabled, to help differentiate if an SET momentarily activated the device under the heavy-ion irradiation. During SEB/SEGR testing with the device "disabled," no V_{OUT} transient or input

current events were observed. No SEB/SEGR events were observed during all four runs, indicating that the TPS7H4010-SEP is SEB/SEGR-free up to $LET_{EFF} = 43 \text{ MeV}\cdot\text{cm}^2/\text{mg}$ and across the full electrical specifications. Table 8-2 shows the SEB test conditions and results. Figure 8-2 shows a plot of the current vs time for run # 5 (Enabled) and Figure 8-3 for run # 6 (Disabled).

Table 8-2. Summary of TPS7H4010-SEP SEB Test Condition and Results

RUN #	UNIT #	ION	LET_{EFF} (MeV·cm ² /mg)	FLUX (ions·cm ² ·s)	FLUENCE (# ions)	V _{OUT} (V)	ENABLED STATUS
5	5	⁸⁴ Kr	43	1.05×10^5	1×10^7	1.8	Enabled
6	5	⁸⁴ Kr	43	1.06×10^5	9.99×10^6	1.8	Disabled
7	6	⁸⁴ Kr	43	1.12×10^5	9.95×10^6	3.3	Enabled
46	6	⁸⁴ Kr	43	1.24×10^5	1×10^7	3.3	Disabled

Using the MFTF method described in [Single-Event Effects \(SEE\) Confidence Interval Calculations application report](#) and combining (or summing) the fluences of the four runs @ 10°C (3.06×10^7), the upper-bound cross-section (using a 95% confidence level) is calculated as:

$$\sigma_{SEB} \leq 1.21 \times 10^{-7} \text{ cm}^2/\text{device} \text{ for } LET_{EFF} = 43 \text{ MeV}\cdot\text{cm}^2/\text{mg} \text{ and } T = 10^\circ\text{C}.$$

The current spikes are due to the output transients on the output voltage.

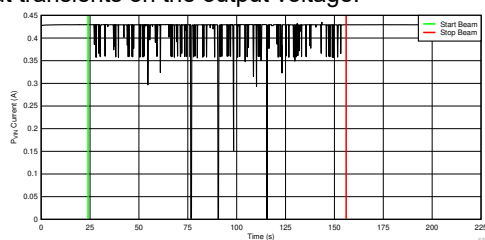


Figure 8-2. Current vs Time for Run # 5 (Enabled) for the TPS7H4010-SEP at T = 10°C

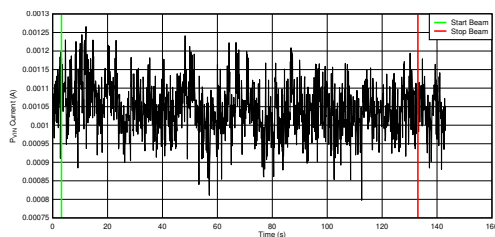


Figure 8-3. Current vs Time for Run # 6 (Disabled) for the TPS7H4010-SEP at T = 10°C

9 Single-Event Transients (SET)

SETs are defined as heavy-ion-induced transients upsets on the V_{OUT} and the PGOOD flag of the TPS7H4010-SEP. SET testing was performed at room temperature (no external temperature control applied). The species used for the SET testing was ^{84}Kr , ^{63}Cu , ^{40}Ar , ^{20}Ne , and ^{14}N for a range of $\text{LET}_{\text{EFF}} = 1.33$ to $43 \text{ MeV}\cdot\text{cm}^2/\text{mg}$, for more details refer to [Section 6](#). Flux of approximately $10^4 \text{ ions}/\text{cm}^2\cdot\text{s}$ and a fluence of approximately $3 \times 10^6 \text{ ions}/\text{cm}^2$ were used for the SET runs.

V_{OUT} SETs were characterized using a window trigger of $\pm 3\%$ around the nominal output voltage (≈ 1.8 and 3.3 V). The devices were characterized at $P_{VIN} = 5 \text{ V}$ (for $V_{OUT} = 1.8 \text{ V}$) and $P_{VIN} = 12 \text{ V}$ (for $V_{OUT} = 3.3 \text{ V}$). The output load was set to 6 A for both runs by using discrete power resistors of 0.55Ω (for $V_{OUT} = 3.3 \text{ V}$) and 0.3Ω (for $V_{OUT} = 1.8 \text{ V}$). To capture the SETs two NI-PXI-5172 scope card were used to continuously monitor the V_{OUT} and the PGOOD. Each scope was operated independently from each other. The output voltage was monitored by using the TP1 and the TP15 test points on the EVM, while the PGOOD was monitored using the TP11 and TP25 test points. The scope triggering from PGOOD was also monitoring the output voltage. The PGOOD and V_{OUT} were tied together through a $100\text{-k}\Omega$ resistor (pull-up).

The scope triggering from V_{OUT} was programmed to record 80k samples with a sample rate of 10 M samples per second (S/s) in case of an event (trigger). The scope triggering from PGOOD was programmed with 30k samples and 5 MS/s . Both scopes were programmed to record 20% of the data before the trigger occurred.

Under heavy-ions, the TPS7H4010-SEP exhibits three transient upsets that were fully recoverable without the need for external intervention. Two distinct signatures were observed on the output voltage.

1. A fast transient of both polarities (positive and negative) with typical deviation of $\approx 4.3\%$ and transient times of $\approx 30 \mu\text{s}$. This transients are referred here as V_{OUT_SET} .
2. A slow transient that drops to zero volts and recover within the programmed soft start time, refer here as SS_{SEFI} .

The SS_{SEFI} is associated with a disturbance on the soft start circuit. During the SS_{SEFI} the soft start circuit discharges the SS capacitor (through an internal FET) and restarted the device. Since no external soft start capacitor was used on the EVM, the internal soft start time of $\approx 6 \text{ ms}$ was observed during this kind of SS_{SEFI} . PGOOD SETs at trigger levels of 300 mV below the nominal output voltage were observed. Since the PGOOD was pulled-up to the output voltage; with each transient on V_{OUT} that droops 300 mV a capture was initiated on the scope triggering from the PGOOD signal. However this was not a real transient on the PGOOD circuit. Since PGOOD circuit is designed to pull-down when the output voltage is not within 10% of the final value, each $V_{OUT_SET} > |10\%|$ was also captured on the scope triggering from PGOOD. All the data that was captured on this scope was processed to eliminate the intrinsic electronic behavior and the coupling with the output voltage. Those SETs that were true transients on the PGOOD circuitry were compared to half the nominal output voltage. This is valid since PGOOD is typically connected to digital circuits with $V_{IL} = 200 \text{ mV}$. After processing, there were no captures for PGOOD that met this condition. Weibull FITs were conducted for each output case (1.8V and 3.3V) as well as each transient type (V_{OUT_SET} and SS_{SEFI}). The weibull parameters and FIT plots are shown in table 9-5 and figure 9-1.

Test conditions and results are summarized in [Table 9-1](#). Histograms for the V_{OUT_SET} peak normalized deviation and the transient time for run # 9 and # 10 are shown from [Figure 9-2](#) to [Figure 9-5](#), since all the SS_{SEFI} drop to zero. Only the Tt histogram is shown in [Figure 9-6](#) and [Figure 9-7](#). [Figure 9-8](#) to [Figure 9-13](#) show typical time domain plots for all the different types of the observed SETs for $V_{OUT} = 1.8 \text{ V}$ and $V_{OUT} = 3.3 \text{ V}$.

Table 9-1. Summary of TPS7H4010-SEP SET Test Condition and Results ($V_{IN} = 5\text{V}$ and $V_{OUT} = 1.8\text{V}$)

RUN #	UNIT #	ION	LET_{EFF} ($\text{MeV}\cdot\text{cm}^2/\text{mg}$)	FLUX ($\text{ions}\cdot\text{cm}^2\cdot\text{s}$)	FLUENCE (# ions)	V_{OUT_SET} (#) $\geq 3\% $	SS_{SEFI} (#)	PGOOD SET $\leq V_{OUT} / 2$
9	7	^{84}Kr	43	1.17×10^4	3×10^6	686	216	0
10	9	^{84}Kr	43.1	1.18×10^4	3×10^6	251	248	0
11	9	^{84}Kr	29.7	1.09×10^4	2.99×10^6	192	166	0
12	9	^{63}Cu	28.1	1.07×10^4	3×10^6	174	165	0
13	9	^{63}Cu	19.7	1.08×10^4	2.99×10^6	184	159	0

Table 9-1. Summary of TPS7H4010-SEP SET Test Condition and Results ($V_{IN} = 5V$ and $V_{OUT} = 1.8V$) (continued)

RUN #	UNIT #	ION	LET _{EFF} (MeV·cm ² /mg)	FLUX (ions·cm ² ·s)	FLUENCE (# ions)	VOUT _{SET} (#) ≥ 3%	SS _{SEFI} (#)	PGOOD SET ≤ V _{OUT} / 2
14	9	⁴⁰ Ar	12	1.22 x 10 ⁴	2.99 × 10 ⁶	187	72	0
15	9	⁴⁰ Ar	8.44	1.18 x 10 ⁴	2.99 × 10 ⁶	153	22	0
16	9	⁴⁰ Ar	8.44	1.07 x 10 ⁴	3 × 10 ⁶	150	19	0
17	9	²⁰ Ne	3.89	1.12 x 10 ⁴	3 × 10 ⁶	92	11	0
18	9	²⁰ Ne	2.74	1.11 x 10 ⁴	2.99 × 10 ⁶	43	5	0
19	9	¹⁴ N	1.33	1.11 x 10 ⁴	2.99 × 10 ⁶	18	0	0

Table 9-2. Summary of TPS7H4010-SEP SET Test Condition and Results ($V_{IN} = 12V$ & $V_{OUT} = 3.3V$)

Run #	Unit #	ION	LET _{EFF} (MeV·cm ² /mg)	FLUX (ions·cm ² ·s)	FLUENCE (# ions)	VOUT _{SET} (#) ≥ 3%	SS _{SEFI} (#)	PGOOD SET ≤ V _{OUT} / 2
20	8	⁸⁴ Kr	43	1.05 x 10 ⁴	3 × 10 ⁶	251	218	0
21	10	⁸⁴ Kr	43.1	1.28 x 10 ⁴	3 × 10 ⁶	448	189	0
22	10	⁸⁴ Kr	29.7	1.03 x 10 ⁴	2.99 × 10 ⁶	362	167	0
23	10	⁶³ Cu	28.1	9.16 x 10 ³	2.99 × 10 ⁶	398	178	0
24	10	⁶³ Cu	19.7	1.28 x 10 ⁴	3 × 10 ⁶	322	145	0
25	10	⁴⁰ Ar	12	1.28 x 10 ⁴	2.99 × 10 ⁶	301	82	0
26	10	⁴⁰ Ar	8.44	1.28 x 10 ⁴	2.99 × 10 ⁶	189	31	0
27	10	²⁰ Ne	3.89	1.13 x 10 ⁴	3 × 10 ⁶	108	6	0
28	10	²⁰ Ne	2.74	1.12 x 10 ⁴	3 × 10 ⁶	84	12	0
29	10	¹⁴ N	1.33	9.07 x 10 ³	2.99 × 10 ⁶	24	0	0

Using the MFTF method described in [Single-Event Effects \(SEE\) Confidence Interval Calculations application report](#), the upper-bound cross-section (using a 95% confidence level) is calculated for the different SETs as shown in [Table 9-3](#) and [Table 9-4](#).

Table 9-3. Upper Bound Cross Section for $V_{OUT} = 1.8 V$ at 95% Confidence Interval and Room Temperature

Run #	SET TYPE	# UPSETS	UPPER BOUND CROSS SECTION (cm ² /device)	SET TYPE	# UPSETS	UPPER BOUND CROSS SECTION (cm ² /device)	SET TYPE	# UPSETS	UPPER BOUND CROSS SECTION (cm ² /device)
9	VOUT _{SET} ≥ 3%	686	2.46 × 10 ⁻⁴	SS _{SEFI}	216	8.23 × 10 ⁻⁵	PGOOD ≤ 0.9 – V	0	1.23 × 10 ⁻⁶
10	VOUT _{SET} ≥ 3%	251	9.47 × 10 ⁻⁵	SS _{SEFI}	248	9.36 × 10 ⁻⁵	PGOOD ≤ 0.9 – V	0	1.23 × 10 ⁻⁶
11	VOUT _{SET} ≥ 3%	192	7.40 × 10 ⁻⁵	SS _{SEFI}	166	6.45 × 10 ⁻⁵	PGOOD ≤ 0.9 – V	0	1.23 × 10 ⁻⁶
12	VOUT _{SET} ≥ 3%	174	6.74 × 10 ⁻⁵	SS _{SEFI}	165	6.41 × 10 ⁻⁵	PGOOD ≤ 0.9 – V	0	1.23 × 10 ⁻⁶
13	VOUT _{SET} ≥ 3%	184	7.11 × 10 ⁻⁵	SS _{SEFI}	159	6.21 × 10 ⁻⁵	PGOOD ≤ 0.9 – V	0	1.23 × 10 ⁻⁶
14	VOUT _{SET} ≥ 3%	187	7.22 × 10 ⁻⁵	SS _{SEFI}	72	3.03 × 10 ⁻⁵	PGOOD ≤ 0.9 – V	0	1.23 × 10 ⁻⁶

Table 9-3. Upper Bound Cross Section for $V_{OUT} = 1.8\text{ V}$ at 95% Confidence Interval and Room Temperature (continued)

Run #	SET TYPE	# UPSETS	UPPER BOUND CROSS SECTION (cm ² /device)	SET TYPE	# UPSETS	UPPER BOUND CROSS SECTION (cm ² /device)	SET TYPE	# UPSETS	UPPER BOUND CROSS SECTION (cm ² /device)
15	$V_{OUT_{SET}} \geq 3\% $	153	6.00×10^{-5}	SS _{SEFI}	22	1.11×10^{-5}	PGOOD $\leq 0.9 - V$	0	1.23×10^{-6}
16	$V_{OUT_{SET}} \geq 3\% $	150	5.87×10^{-5}	SS _{SEFI}	19	9.89×10^{-6}	PGOOD $\leq 0.9 - V$	0	1.23×10^{-6}
17	$V_{OUT_{SET}} \geq 3\% $	92	3.76×10^{-5}	SS _{SEFI}	11	6.56×10^{-6}	PGOOD $\leq 0.9 - V$	0	1.23×10^{-6}
18	$V_{OUT_{SET}} \geq 3\% $	43	1.94×10^{-5}	SS _{SEFI}	5	3.90×10^{-6}	PGOOD $\leq 0.9 - V$	0	1.23×10^{-6}
19	$V_{OUT_{SET}} \geq 3\% $	18	9.51×10^{-6}	SS _{SEFI}	0	1.23×10^{-6}	PGOOD $\leq 0.9 - V$	0	1.23×10^{-6}

Table 9-4. Upper Bound Cross Section for $V_{OUT} = 3.3\text{ V}$ at 95% Confidence Interval and Room Temperature

Run #	SET TYPE	# UPSETS	UPPER BOUND CROSS SECTION (cm ² /device)	SET TYPE	# UPSETS	UPPER BOUND CROSS SECTION (cm ² /device)	SET TYPE	# UPSETS	UPPER BOUND CROSS SECTION (cm ² /device)
20	$V_{OUT_{SET}} \geq 3\% $	251	9.47×10^{-5}	SS _{SEFI}	218	8.3×10^{-5}	PGOOD $\leq 0.9 - V$	0	1.23×10^{-6}
21	$V_{OUT_{SET}} \geq 3\% $	448	1.54×10^{-4}	SS _{SEFI}	189	7.25×10^{-5}	PGOOD $\leq 0.9 - V$	0	1.23×10^{-6}
22	$V_{OUT_{SET}} \geq 3\% $	362	1.34×10^{-4}	SS _{SEFI}	167	6.50×10^{-5}	PGOOD $\leq 0.9 - V$	0	1.23×10^{-6}
23	$V_{OUT_{SET}} \geq 3\% $	398	1.47×10^{-4}	SS _{SEFI}	178	6.89×10^{-5}	PGOOD $\leq 0.9 - V$	0	1.23×10^{-6}
24	$V_{OUT_{SET}} \geq 3\% $	322	1.20×10^{-4}	SS _{SEFI}	145	5.69×10^{-5}	PGOOD $\leq 0.9 - V$	0	1.23×10^{-6}
25	$V_{OUT_{SET}} \geq 3\% $	301	1.13×10^{-4}	SS _{SEFI}	82	3.40×10^{-5}	PGOOD $\leq 0.9 - V$	0	1.23×10^{-6}
26	$V_{OUT_{SET}} \geq 3\% $	189	7.29×10^{-5}	SS _{SEFI}	31	1.47×10^{-5}	PGOOD $\leq 0.9 - V$	0	1.23×10^{-6}
27	$V_{OUT_{SET}} \geq 3\% $	108	4.35×10^{-5}	SS _{SEFI}	6	4.35×10^{-6}	PGOOD $\leq 0.9 - V$	0	1.23×10^{-6}
28	$V_{OUT_{SET}} \geq 3\% $	84	3.46×10^{-5}	SS _{SEFI}	12	6.98×10^{-6}	PGOOD $\leq 0.9 - V$	0	1.23×10^{-6}
29	$V_{OUT_{SET}} \geq 3\% $	24	1.19×10^{-5}	SS _{SEFI}	0	1.23×10^{-6}	PGOOD $\leq 0.9 - V$	0	1.23×10^{-6}

Table 9-5. Weibull Parameters for $V_{OUT} = 1.8\text{V}$ and 3.3V Cases

Parameters	1.8V $V_{OUT_{SET}}$	1.8V SS _{SEFI}	3.3V $V_{OUT_{SET}}$	3.3 SS _{SEFI}
Upper Bound Cross Section (cm ²)	9.47×10^{-5}	9.36×10^{-5}	1.64×10^{-4}	7.27×10^{-5}
Cross-Saturation (cm ²)	8.37×10^{-5}	8.27×10^{-5}	1.49×10^{-4}	6.3×10^{-5}
Onset (MeV·cm ² /mg)	1	1.33	1	1.33
w	11	20	12	16

Table 9-5. Weibull Parameters for $V_{OUT} = 1.8V$ and $3.3V$ Cases (continued)

Parameters	1.8V V_{OUT_SET}	1.8V SS_{SEFI}	3.3V V_{OUT_SET}	3.3V SS_{SEFI}
s	1	1.6	1	2.2

X-axis is LET_{EFF} and Y-axis is respective upper bound cross section.

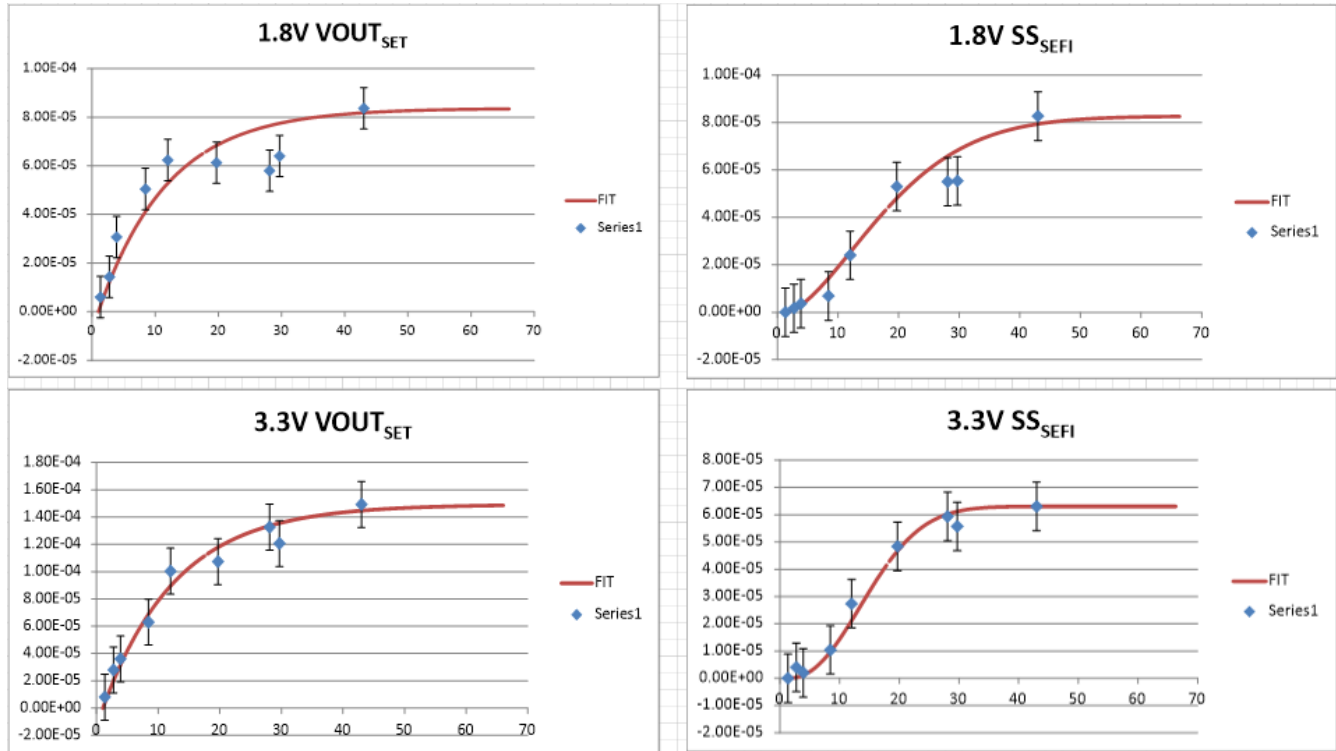


Figure 9-1. Weibull FITs for each V_{OUT} case

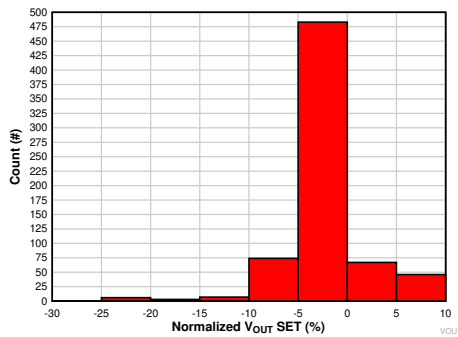


Figure 9-2. Histogram of the Normalized Amplitude for the Positive and Negative V_{OUT} SETs on Run # 9

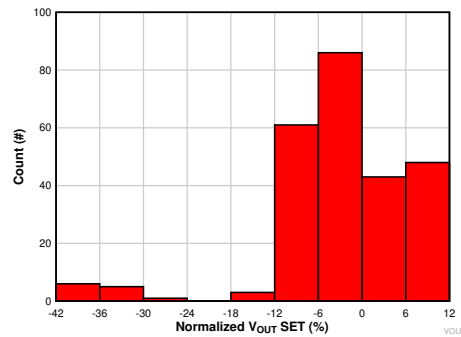


Figure 9-3. Histogram of the Normalized Amplitude for the Positive and Negative V_{OUT} SETs on Run # 10

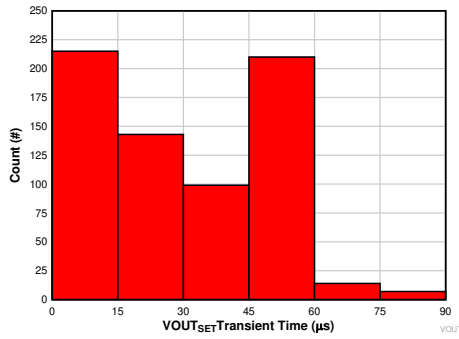


Figure 9-4. Histogram of the Transient Time for V_{OUT} SETs on Run # 9

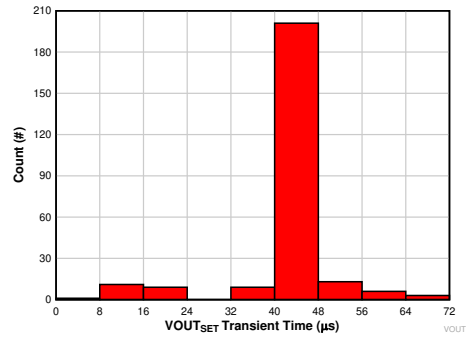


Figure 9-5. Histogram of the Transient Time for V_{OUT} SETs on Run # 10

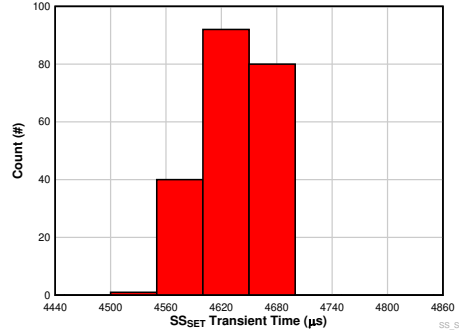


Figure 9-6. Histogram of the Transient Time for SS SETs on Run # 9

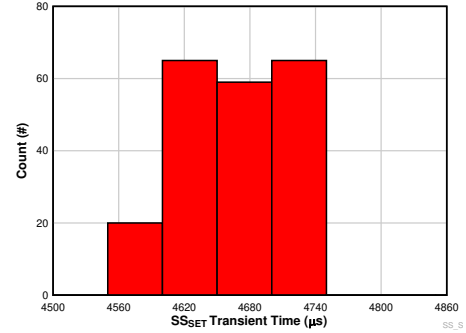


Figure 9-7. Histogram of the Transient Time for SS SETs on Run # 10

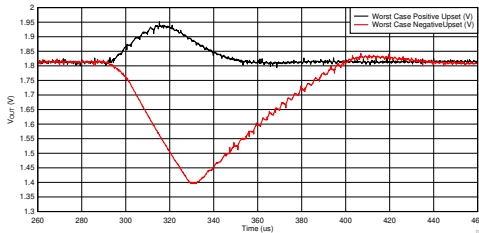


Figure 9-8. Worst Case Positive and Negative Polarity V_{OUTSET} for Run # 9

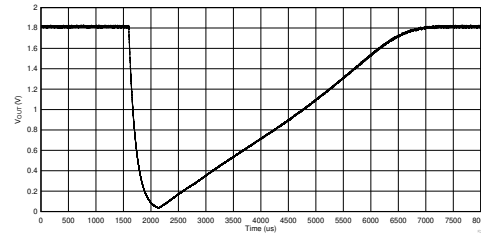


Figure 9-9. Typical V_{OUT} During a SS_{SEFI} for Run # 9

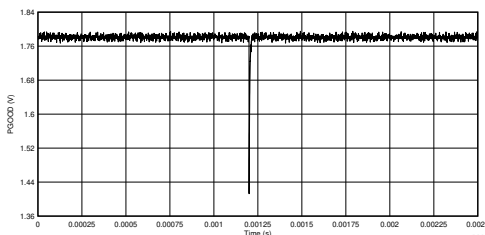


Figure 9-10. Typical $PGOOD_{SET} \leq 0.9$ V for Run # 9

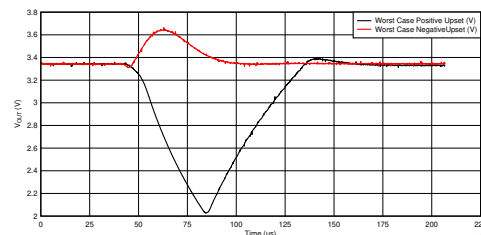


Figure 9-11. Worst Case Positive and Negative Polarity V_{OUTSET} for Run # 10

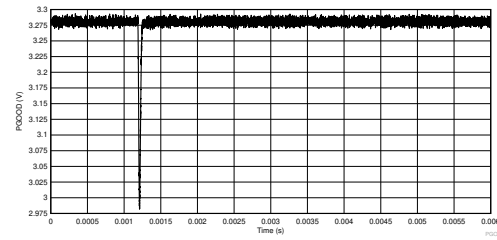
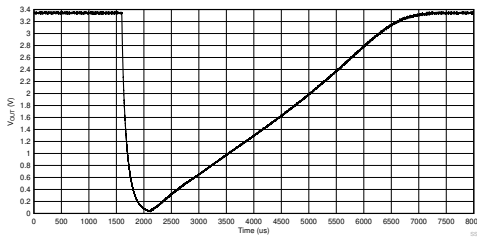


Figure 9-12. Typical V_{OUT} During a SS_{SET} for Run # 10 **Figure 9-13. Typical $PGOOD_{SET} \leq 1.6$ V for Run # 10**

10 Event Rate Calculations

Event rates were calculated for LEO(ISS) and GEO environments by combining CREME96 orbital integral flux estimations and simplified SEE cross-sections according to methods described in [Heavy Ion Orbital Environment Single-Event Effects Estimations application report](#). We assume a minimum shielding configuration of 100 mils (2.54 mm) of aluminum, and “worst-week” solar activity (this is similar to a 99% upper bound for the environment). Using the 95% upper-bounds for the SEL and the SEB/SEGR, the event rate calculation for the SEL and the SEB/SEGR is shown on [Table 10-1](#) and [Table 10-2](#), respectively. **It is important to note that this number is for reference since no SEL or SEB/SEGR events were observed.**

Table 10-1. SEL Event Rate Calculations for Worst-Week LEO and GEO Orbits

Orbit Type	Onset LET_{EFF} (MeV-cm ² /mg)	CREME96 Integral FLUX (/day/cm ²)	σ_{SAT} (cm ²)	Event Rate (/day)	Event Rate (FIT)	MTBE (Years)
LEO (ISS)	43	6.4×10^{-4}	9.23×10^{-8}	5.91×10^{-11}	2.5×10^{-3}	4.63×10^7
GEO		2.2×10^{-3}		2×10^{-10}	8.4×10^{-3}	1.36×10^7

Table 10-2. SEB/SEGR Event Rate Calculations for Worst-Week LEO and GEO Orbits

Orbit Type	Onset LET_{EFF} (MeV-cm ² /mg)	CREME96 Integral FLUX (/day/cm ²)	σ_{SAT} (cm ²)	Event Rate (/day)	Event Rate (FIT)	MTBE (Years)
LEO (ISS)	43	6.4×10^{-4}	1.21×10^{-7}	7.74×10^{-11}	3.2×10^{-3}	3.53×10^7
GEO		2.2×10^{-3}		2.62×10^{-10}	11×10^{-3}	1.04×10^7

Table 10-3. Combined SET (1.8V) Event Rate Calculations for Worst-Week LEO and GEO Orbits

Orbit Type	Onset LET_{EFF} (MeV-cm ² /mg)	CREME96 Integral FLUX (/day/cm ²)	σ_{SAT} (cm ²)	Event Rate (/day)	Event Rate (FIT)	MTBE (Years)
LEO (ISS)	1	2.24×10^3	1.66×10^{-4}	3.72×10^{-1}	1.55×10^7	7.36×10^{-3}
GEO		2.70×10^4		4.49×10^0	1.87×10^8	6.10×10^{-4}

Table 10-4. V_{OUT} SET (1.8V) Event Rate Calculations for Worst-Week LEO and GEO Orbits

Orbit Type	Onset LET_{EFF} (MeV-cm ² /mg)	CREME96 Integral FLUX (/day/cm ²)	σ_{SAT} (cm ²)	Event Rate (/day)	Event Rate (FIT)	MTBE (Years)
LEO (ISS)	1	2.24×10^3	8.37×10^{-5}	1.87×10^{-1}	7.81×10^6	1.46×10^{-2}
GEO		2.70×10^4		2.26×10^0	9.42×10^7	1.21×10^{-3}

Table 10-5. SS SEFI (1.8V) Event Rate Calculations for Worst-Week LEO and GEO Orbits

Orbit Type	Onset LET_{EFF} (MeV-cm ² /mg)	CREME96 Integral FLUX (/day/cm ²)	σ_{SAT} (cm ²)	Event Rate (/day)	Event Rate (FIT)	MTBE (Years)
LEO (ISS)	2	5.25×10^2	8.27×10^{-5}	4.34×10^{-2}	1.81×10^6	6.31×10^{-2}
GEO		5.22×10^3		4.31×10^{-1}	1.80×10^7	6.35×10^{-3}

Table 10-6. Combined SET (3.3V) Event Rate Calculations for Worst-Week LEO and GEO Orbits

Orbit Type	Onset LET _{EFF} (MeV-cm ² /mg)	CREME96 Integral FLUX (/day/cm ²)	σSAT (cm ²)	Event Rate (/day)	Event Rate (FIT)	MTBE (Years)
LEO (ISS)	1	2.24 x 10 ³	1.49 x 10 ⁻⁴	3.34 x 10 ⁻¹	1.39 x 10 ⁷	8.20 x 10 ⁻³
GEO		2.70 x 10 ⁴		4.03 x 10 ⁰	1.68 x 10 ⁸	6.79 x 10 ⁻⁴

Table 10-7. VOUT SET (3.3V) Event Rate Calculations for Worst-Week LEO and GEO Orbits

Orbit Type	Onset LET _{EFF} (MeV-cm ² /mg)	CREME96 Integral FLUX (/day/cm ²)	σSAT (cm ²)	Event Rate (/day)	Event Rate (FIT)	MTBE (Years)
LEO (ISS)	1	2.24 x 10 ³	8.63 x 10 ⁻⁵	1.93 x 10 ⁻¹	8.05 x 10 ⁶	1.42 x 10 ⁻²
GEO		2.70 x 10 ⁴		2.33 x 10 ⁰	9.71 x 10 ⁷	1.18 x 10 ⁻³

Table 10-8. SS SEFI (3.3V) Event Rate Calculations for Worst-Week LEO and GEO Orbits

Orbit Type	Onset LET _{EFF} (MeV-cm ² /mg)	CREME96 Integral FLUX (/day/cm ²)	σSAT (cm ²)	Event Rate (/day)	Event Rate (FIT)	MTBE (Years)
LEO (ISS)	2	5.25 x 10 ²	6.30 x 10 ⁻⁵	3.31 x 10 ⁻²	1.38 x 10 ⁶	8.28 x 10 ⁻²
GEO		5.22 x 10 ³		3.29 x 10 ⁻¹	1.37 x 10 ⁷	8.34 x 10 ⁻³

11 Summary

The purpose of this study was to characterize the effect of heavy-ion irradiation on the single-event effect (SEE) performance of the TPS7H4010-SEP synchronous step-down POL converter. Heavy-ions with $LET_{EFF} = 43 \text{ MeV}\cdot\text{cm}^2/\text{mg}$ were used for the SEE characterization campaign. Flux of 10^4 and 10^5 ions/ $\text{cm}^2\cdot\text{s}$ and fluences ranging from 3×10^6 to 1×10^7 ions/ cm^2 per run were used for the characterization. The SEE results demonstrated that the TPS7H4010-SEP POL is free of destructive SEB events and SEL-free up to $LET_{EFF} = 43 \text{ MeV}\cdot\text{cm}^2/\text{mg}$ and across the full electrical specifications. Transients at $LET_{EFF} = 43 \text{ MeV}\cdot\text{cm}^2/\text{mg}$ on V_{OUT} and PGOOD are presented and discussed. CREME96-based worst-week event-rate calculations for LEO(ISS) and GEO orbits for the DSEE are presented for reference.

12 Revision History

NOTE: Page numbers for previous revisions may differ from page numbers in the current version.

Changes from Revision * (December 2020) to Revision A (April 2023)	Page
• Changes made throughout explaining the ions used while testing.....	3

Changes from Revision A (April 2023) to Revision B (November 2024)	Page
• Changes SSET to SSEFI throughout the document.....	3
• Updated to show all ions used during testing.....	10
• Updated Summary of TPS7H4010-SEP SEB Test Condition and Results table	14
• Added Weibull Parameters for $V_{OUT} = 1.8\text{V}$ and 3.3V Cases table.....	16
• Added Weibull FITs for each V_{OUT} case figure.....	16
• Updated Event Rate Calculations table data (added tables 11-3 through 11-8).....	21

A Total Ionizing Dose from SEE Experiments

The production TPS7H4010-SEP POL is rated to a total ionizing dose (TID) of 20 krad(Si). In the course of the SEE testing, the heavy-ion exposures delivered ≈ 10 krad(Si) per 10^7 ions/ cm^2 run. The cumulative TID exposure over all runs was determined to be between 3 krad(Si) to 20 krad(Si), for each device. All eight production TPS7H4010-SEP devices used in the studies described in this report stayed within specification and were fully-functional after the heavy-ion SEE testing was completed.

B References

1. M. Shoga and D. Binder, "Theory of Single Event Latchup in Complementary Metal-Oxide Semiconductor Integrated Circuits", *IEEE Trans. Nucl. Sci.*, Vol. 33(6), Dec. 1986, pp. 1714-1717.
2. G. Bruguier and J. M. Palau, "Single particle-induced latchup", *IEEE Trans. Nucl. Sci.*, Vol. 43(2), Mar. 1996, pp. 522-532.
3. G. H. Johnson, J. H. Hohl, R. D. Schrimpf and K. F. Galloway, "Simulating single-event burnout of n-channel power MOSFET's," in IEEE Transactions on Electron Devices, vol. 40, no. 5, pp. 1001-1008, May 1993.
4. J. R. Brews, M. Allenspach, R. D. Schrimpf, K. F. Galloway, J. L. Titus and C. F. Wheatley, "A conceptual model of a single-event gate-rupture in power MOSFETs," in IEEE Transactions on Nuclear Science, vol. 40, no. 6, pp. 1959-1966, Dec. 1993.
5. G. H. Johnson, R. D. Schrimpf, K. F. Galloway, and R. Koga, "Temperature dependence of single event burnout in n-channel power MOSFETs [for space application]," *IEEE Trans. Nucl. Sci.*, 39(6), Dec. 1992, pp.1605-1612.
6. TAMU Radiation Effects Facility website. <http://cyclotron.tamu.edu/ref/>
7. "The Stopping and Range of Ions in Matter" (SRIM) software simulation tools website. www.srim.org/index.htm#SRIMMENU
8. D. Kececioglu, "Reliability and Life Testing Handbook", Vol. 1, PTR Prentice Hall, New Jersey, 1993, pp. 186-193.
9. ISDE CRÈME-MC website. <https://creme.isde.vanderbilt.edu/CREME-MC>

10. A. J. Tylka, J. H. Adams, P. R. Boberg, et al., "CREME96: A Revision of the Cosmic Ray Effects on Micro-Electronics Code", *IEEE Trans. on Nucl. Sci.*, Vol. 44(6), Dec. 1997, pp. 2150-2160.
11. A. J. Tylka, W. F. Dietrich, and P. R. Boberg, "Probability distributions of high-energy solar-heavy-ion fluxes from IMP-8: 1973-1996", *IEEE Trans. on Nucl. Sci.*, Vol. 44(6), Dec. 1997, pp. 2140-2149.

IMPORTANT NOTICE AND DISCLAIMER

TI PROVIDES TECHNICAL AND RELIABILITY DATA (INCLUDING DATA SHEETS), DESIGN RESOURCES (INCLUDING REFERENCE DESIGNS), APPLICATION OR OTHER DESIGN ADVICE, WEB TOOLS, SAFETY INFORMATION, AND OTHER RESOURCES "AS IS" AND WITH ALL FAULTS, AND DISCLAIMS ALL WARRANTIES, EXPRESS AND IMPLIED, INCLUDING WITHOUT LIMITATION ANY IMPLIED WARRANTIES OF MERCHANTABILITY, FITNESS FOR A PARTICULAR PURPOSE OR NON-INFRINGEMENT OF THIRD PARTY INTELLECTUAL PROPERTY RIGHTS.

These resources are intended for skilled developers designing with TI products. You are solely responsible for (1) selecting the appropriate TI products for your application, (2) designing, validating and testing your application, and (3) ensuring your application meets applicable standards, and any other safety, security, regulatory or other requirements.

These resources are subject to change without notice. TI grants you permission to use these resources only for development of an application that uses the TI products described in the resource. Other reproduction and display of these resources is prohibited. No license is granted to any other TI intellectual property right or to any third party intellectual property right. TI disclaims responsibility for, and you will fully indemnify TI and its representatives against, any claims, damages, costs, losses, and liabilities arising out of your use of these resources.

TI's products are provided subject to [TI's Terms of Sale](#) or other applicable terms available either on [ti.com](https://www.ti.com) or provided in conjunction with such TI products. TI's provision of these resources does not expand or otherwise alter TI's applicable warranties or warranty disclaimers for TI products.

TI objects to and rejects any additional or different terms you may have proposed.

Mailing Address: Texas Instruments, Post Office Box 655303, Dallas, Texas 75265
Copyright © 2024, Texas Instruments Incorporated